JOURNAL OF GEOPHYSICAL RESEARCH, VOL. 102, NO. E8, PAGES 19,307–19,320, AUGUST 25, 1997

Regolith composition and structure in the lunar maria: Results of long-wavelength radar studies

Bruce A. Campbell

Center for Earth and Planetary Studies, Smithsonian Institution, Washington, D.C.

B. Ray Hawke

Department of Planetary Geosciences, University of Hawaii, Honolulu

Thomas W. Thompson

Jet Propulsion Laboratory, Pasadena, California

Abstract. Radar measurements at 70-cm and 7.5-m wavelengths provide insight into the structure and composition of the upper 5–100 m of the lunar regolith and crust. We combine high-resolution (3-5 km) 70-cm radar data for the nearside with earlier calibrated full-disk observations at the same wavelength to provide a reasonable estimate of the lunar backscatter coefficient. These data are tested against models for echoes from a buried substrate and Mie scattering from surface and buried rocks. These mechanisms are expected to dominate the 70-cm radar echo, with their relative importance determined by the rock population, regolith depth, substrate roughness, and the loss tangent of the soil. Results indicate that the 70-cm radar echo for the maria comes largely from Mie scattering by rocks buried within the fine soil. Radar scattering from a buried substrate is not likely to greatly affect the observed return. We also compared the 70-cm and 7.5-m radar images to infrared eclipse temperature maps, crater-population age estimates for the maria, and to TiO_2 and FeO abundances inferred from Earth-based telescopic and Clementine multispectral observations. These data imply that (1) the TiO_2 (ilmenite) content of the regolith controls variations in 70-cm depolarized echo strength among mare units, with higher titanium abundance leading to lower echoes; (2) changes in the average 70-cm return for a given TiO_2 abundance between maria of different ages do occur, but uncertainties in the current radar data do not allow us to uniquely distinguish between variations in rock population with age and calibration effects; (3) the 7.5-m radar echoes are controlled by the age of the mare basalt flows, with older deposits having a greater degree of fracturing and higher backscatter. Future mapping at 12.6-cm and 70-cm wavelengths will help to resolve some of the issues raised here.

Introduction

The composition and structure of the lunar regolith are of fundamental importance to the geologic study of the Moon. The regolith is a mixture of fine soil particles, glass-bonded agglutinates, and a variety of mineral and lithic fragments, all formed by impact bombardment, which overlies the fractured lava flows in the maria and basin- and crater-related deposits in the highlands. The majority of the included rocks are locally derived from the bedrock underlying the regolith, but some fraction have been transported from distant areas by large impacts. The regolith is estimated to be 3-8 m deep in the maria [*Horz et al.*, 1991; *Moore et al.*, 1980], and in vertical section is a complex assortment of thin layers produced by impact craters and subsequent micrometeorite gardening. Over large areas, it is expected that these layers are not coherent, and that any stratification in the soil is localized and highly variable.

Paper number 97JE00858.
0148-0227/97/97JE-00858$09.00

Apollo core samples, seismic data, and the lunar sounder experiment provided some information regarding the physical bounds on regolith depth and grain size, but the variability of soil properties across the Moon is not well understood. Most of the compositional information for the regolith comes from spectral ratio parameters and orbital geochemistry data that have been calibrated to measured values for the Apollo and Luna landing sites. The primary interest in remote mare soil studies is a determination of their bulk oxide content, which is dominated by SiO_2, FeO, TiO_2, Al_2O_3, MgO, and CaO [*Papike et al.*, 1991]. These elements are found in minerals such as olivine, pyroxene, and ilmenite ($FeTiO_3$), and their abundances vary across the maria due to lateral differences in magma source regions and fractionation histories. Knowledge of the abundance of these elements thus provides important information concerning the formational history of the upper lunar crust.

Radar scattering at oblique incidence angles (>20°) from the regolith can arise from several sources, whose importance varies with the wavelength, λ, of the probing energy. Surface rocks and regolith sculpture will be the primary scatterers at X-band wavelengths (3 cm), while larger blocks and those buried

in the soil become progressively more important at S (12 cm) and P (70 cm) bands. Finally, any strong dielectric boundary, such as between the soil and a rock basement, will make a contribution if the radar energy is not attenuated prior to encountering the bedrock interface. Imaging radar data for the Moon have often been used as a tool for characterizing the regolith, particularly in the study of crater ejecta distribution and large pyroclastic deposits [e.g., *Zisk et al.*, 1977; *Thompson et al.*, 1979; *Moore et al.*, 1980; *Gaddis et al.*, 1985]. Much of this work utilized the 3.8-cm radar maps of *Zisk et al.* [1974], whose 2-km resolution and sensitivity to surface roughness delineate numerous subtle features. The 70-cm data typically were of much lower spatial resolution, but several studies have been made of possible echo sources and the role of regolith properties.

Schaber et al. [1975] determined that the lava flows mapped in Mare Imbrium, which vary widely in their TiO_2 abundance, showed a strong degree of correlation with unit boundaries in the 70-cm data available at the time (5-10 km resolution), and that higher titanium abundances are linked to lower radar echo strength. Work by *Thompson et al.* [1970] *and Pollack and Whitehill* [1972] led to a concensus that the 70-cm radar echoes came largely from rocks buried within the fine soil of the regolith, and that changes in the backscatter strength were due to shifts in the loss tangent of the fine fraction. The loss tangent, in turn, was linked to the titanium and iron content of the material, and laboratory studies of returned samples (summarized by *Carrier et al.* [1991]) supported these hypotheses. To date, however, there have been no efforts to test the 70-cm data as a possible nearside compositional mapping tool, and questions regarding the radar scattering mechanisms remain. To a large degree this work was hampered by a lack of calibrated 70-cm images for the entire nearside, but the 3-5 km resolution map of *Thompson* [1987] overcame this problem using a low-resolution beam-swing technique. The 7.5-m data have been discussed only in the original report by *Thompson* [1978], which presented evidence that the primary echoes were coming from rock layers beneath the regolith.

The spectral reflectance of the lunar soil is controlled by the mineralogy of the original material, the degree of maturation, and by the degree of contamination of the surface layer by impact debris from other geologic units. Since the depth of penetration for reflected visible/near-IR energy is only a few microns, surficial effects dominate the observed spectrum. A number of methodologies have evolved to provide estimates of elemental abundance from this type of remote sensing data. An early application of color variability in soils was carried out by *Whitaker* [1972], who showed that a red-blue (0.37/0.61 μm) ratio image suppressed albedo changes and revealed spectral variations within the maria [see also *Wilhelms*, 1987]. *Charette et al.* [1974] found that the 0.40/0.56 μm ratio for mature mare units correlated with the TiO_2 abundance determined for the returned samples, and proposed an empirical model for extending this relationship to other mature mare soils. Subsequent analysis by *Pieters* [1978] used four major criteria, including the 0.40/0.56 μm ratio, to classify and map the distribution of a number of basalt units on the lunar nearside. This approach is less reliable at lower TiO_2 abundance, where the spectral ratio parameter is more sensitive to other regolith components such as iron [*Pieters*, 1978; *Johnson et al.*, 1991; *Pieters et al.*, 1993; *Melendrez et al.*, 1994]. The constraint on soil maturity is very strict, since immature mare material or highlands contamination will have a major impact on the 0.40/0.56 μm ratio. *Johnson et al.* [1991] mapped the TiO_2 values for the lunar nearside using the Charette relationship at a resolution of ~5 km, and the digital versions of these maps are used here. Methods for determining FeO and TiO_2 abundances from Clementine 0.415, 0.750, and 0.950 μm data, which include the effects of soil maturity, have been developed by *Lucey et al.* [1995; 1996], and their 7-15 km-resolution maps will also be used as a comparison to the radar data. The Apollo gamma ray spectrometer data have also been used to estimate Fe and Ti bulk abundances [*Davis*, 1980], but the spatial coverage and resolution of these maps is rather low (~100 km).

An interesting aspect of the radar data is the fact that they depth-average the properties of the regolith over a significant path length. Where a thin layer of immature soil or highland contaminant (a crater ray, for example) can drastically affect the spectral reflectance of a surface, to the long-wavelength radar this constitutes a small fraction of the total volume which contributes to the echo. This difference in sensitivities suggests that the optical and radar data can offer complementary information. Past work has shown that the 70-cm observations may be a useful tool for mapping compositional changes on the lunar surface, but significant issues in the nature of the scattering need to be addressed. In this paper, we first examine possible sources for the long-wavelength backscatter, and compare the observational data with theoretical models to constrain the range of potential regolith structure. We then compare the 70-cm and 7.5-m data to the results of multispectral mapping of elemental abundances, and consider the implications of these results for the composition and structure of the mare regolith.

Models for Radar Scattering From the Lunar Regolith

The 70-cm maps used here, which have a spatial resolution of 3-5 km, were collected in 1981-1984 at the Arecibo Observatory, and are shown in Plate 1 [*Thompson*, 1987]. In contrast to previous mosaics at this wavelength, which were hampered by a lack of calibration between individual images, the current image was assembled using a low-resolution beam-swing technique to provide a global reference map for radar brightness. To compare these data to the results of theoretical models, we first calibrated the radar images to values of backscatter cross section per unit area (σ^0). This was done by letting the mean polarized (LR: left-circular transmit, right circular receive; also called opposite-sense circular or OC) echo behavior at 70 cm be characterized by the 68-cm lunar average compiled by *Hagfors* [1970]. The depolarized (LL: left-circular transmit, left-circular receive; also called same-sense circular or SC) returns were calibrated by letting the average echoes near the limb be 1/2 (-3 dB) the strength of the polarized component, again as indicated by earlier disk-integrated measurements [*Hagfors*, 1970]. The systematic error in these calibrations is difficult to define, but mosaicking offsets probably produce error bounds of about 1-2 dB between sites in widely separated locales.

A cursory comparison of the 70-cm radar data to color ratio images [i.e., *Whitaker*, 1972] shows that abrupt changes in backscatter cross section within the mare basins are well correlated with spectral-map unit edges indicative of regolith

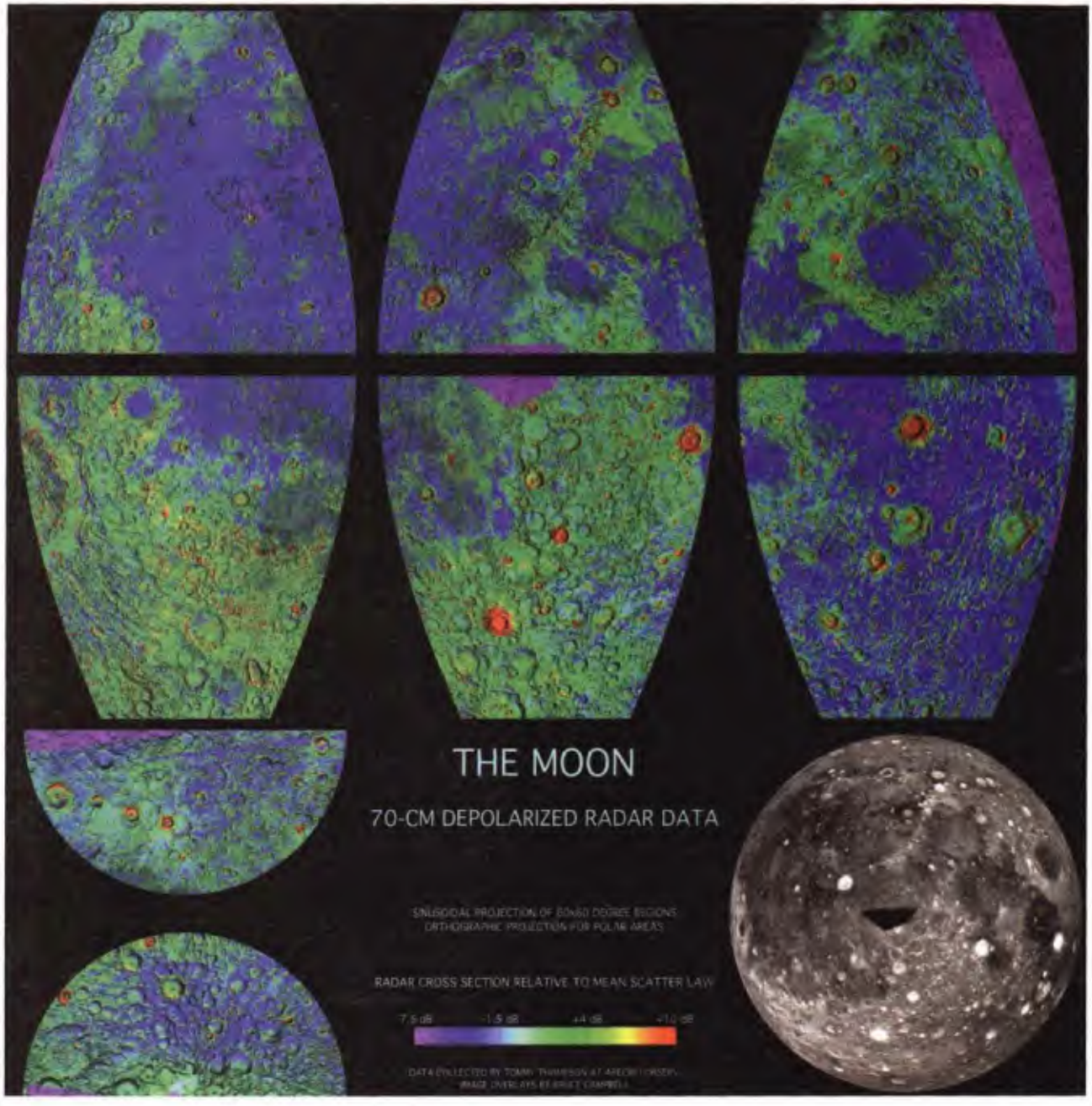

Plate 1. A 70-cm wavelength depolarized radar map of the Moon [from *Thompson*, 1987], overlain on a U.S. Geological Survey shaded-relief image. Image resolution 3-5 km. The depolarized data have been mapped in this figure to six 60°x60° sinusoidal-projection portions of the nearside, and two orthographic maps of the north and south polar regions. The figure at lower right is an orthographic view of the full 70-cm map. Color scale indicates radar backscatter cross section relative to the lunar mean.

chemistry differences [*Schaber et al.*, 1975]. This indicates that the radar data are modulated to a significant degree by the composition of the regolith, but it is interesting to note that the relative echo strength does not simply mirror the spectral ratio values; only the contrast changes tend to be highly correlated. It is thus important to consider the possible sources of radar echoes from the maria, and the way in which these returns are affected by different processes.

The 70-cm radar echoes are influenced to varying degrees by the volumetric rock population, regolith depth, substrate presence and roughness, and the dielectric properties of the rocks and fine soil. To examine the effects of these parameters, we study two major sources of radar returns: echoes from a buried substrate, and Mie scattering from surface and buried rocks. Quasi-specular scattering [*Hagfors*, 1970] is neglected in this analysis because (1) we are interested

primarily in the diffuse component of the echo, which is not produced by large single-scattering facets, and (2) at the angles of interest here (>20°), this mechanism is not the dominant component of the polarized (LR) echo from the relatively smooth (low rms slope) maria.

Buried Substrate Model

This model assumes that a significant portion of the echo comes from a buried scattering layer, characterized by the transition from soil to solid rock, whose depth and roughness vary. In this end-member scenario, no scattering rocks are present in the soil. A simple interface between fine-grained soil and solid rock is, of course, not likely in the lunar regolith. The transition between the two regimes is probably characterized by succeeding layers of rocky debris, fractured and brecciated material, and finally intact lava flows. For our purposes, the base of the regolith is the point at which little further volume scattering can occur, and the underlying rubble behaves as a scattering surface.

The substrate could have a range of scattering behaviors depending upon its roughness, and the measured echo will vary with changes in the microwave loss tangent, defined as the ratio between the imaginary and real components of the complex dielectric constant: $\tan\delta=(\varepsilon''/\varepsilon')$, of the soil. The amount of power, σ^{o}_{obs}, backscattered by a surface buried beneath a layer with a given complex dielectric constant is

$$\sigma^{o}_{obs}(h) = \sigma^{o}_{unm}\, R\, T^2\, e^{-4\,\alpha h / \cos\theta} \tag{1}$$

where the loss factor α is

$$\alpha = \frac{2\pi}{\lambda}\left[\frac{\varepsilon'}{2}\left[\sqrt{1+\tan\delta^2}-1\right]\right]^{0.5} \tag{2}$$

σ^{o}_{unm} is the backscatter cross section of the substrate in the absence of any mantling, h is the depth of the soil layer, λ is the radar wavelength in vacuum, T is a loss factor due to transmission effects at the regolith-space interface, R is a loss factor due to the reduced dielectric contrast at the soil-rock interface relative to that between the rock and free space, and θ is the incidence angle within the soil

$$\theta = \sin^{-1}\left[\frac{\sin\phi}{\sqrt{\varepsilon'}}\right] \tag{3}$$

with the radar incidence angle at the surface given by ϕ [*Ulaby et al.*, 1987]. Transmission effects at the top of the soil layer reduce the observed backscatter, and we estimate the loss factor for a circular-polarized wave as the average of T_h and T_v, the H- and V-polarized Fresnel transmission coefficients (i.e., one-half the power is present in each of the two linear polarizations) [*Stratton*, 1947]:

$$T = \frac{T_h + T_v}{2} = \frac{\sin 2\phi \sin 2\theta}{2\sin^2(\theta+\phi)}\left[1 + \frac{1}{\sin^2(\theta+\phi)\cos^2(\phi-\theta)}\right] \tag{4}$$

For the two-way case of a buried layer this factor must be squared. The polarization effects of the interface due to differences in T_h and T_v are neglected in this treatment. Given the scattering cross-section of a hypothetical substrate, we can thus estimate the observed backscatter echo strength after allowing for transmission and absorption.

The electrical properties of rocks have been studied in detail by a variety of measurement techniques, with good summaries provided by *Ulaby et al.* [1988] for terrestrial samples and by *Carrier et al.* [1991] for lunar rocks. In general, the real part of the dielectric constant is dependent upon rock density, ρ, with little variation due to chemical composition. Lunar soils have real dielectric constants of 2-3, while solid rocks may have values of ε' from 4-8 depending upon their porosity. The imaginary part of the dielectric constant for dry samples is affected by bulk chemistry, with little influence noted for changes in sample density [*Ulaby et al.*, 1988]. For lunar materials, $\tan\delta$ is found to vary by an order of magnitude, from about 0.002 to 0.02, with increasing ($FeO+TiO_2$) values. *Olhoeft and Strangway* [1975] derived a power-law relationship between oxide content, density, and loss tangent at 67 cm wavelength:

$$\tan\delta = 10^{(0.033\,[\%TiO_2 + \%FeO] + 0.231\,\rho - 3.061)} \tag{5}$$

The experimental data have scatter of up to an order of magnitude in $\tan\delta$ about the model fit, so the reliability of the above equation is uncertain. For an average mare FeO content of 12% (*Lucey et al.* [1995]) and regolith density of 1.7 g/cm^3, the predicted loss tangent for zero titanium content is about 0.005.

The change in backscatter strength for a mantled scattering surface is shown in Figure 1 for layer depths of 3-8 m, the expected maximum range of lunar loss tangents, and radar wavelengths of 70 cm and 7.5 m. From these results, we can conclude that the range in 70-cm backscatter echo power for a buried layer with changes in either h or $\tan\delta$ is quite large. At soil depths of more than about 3 m, the range in brightness for loss tangents of 0.005 to 0.02 could exceed that observed

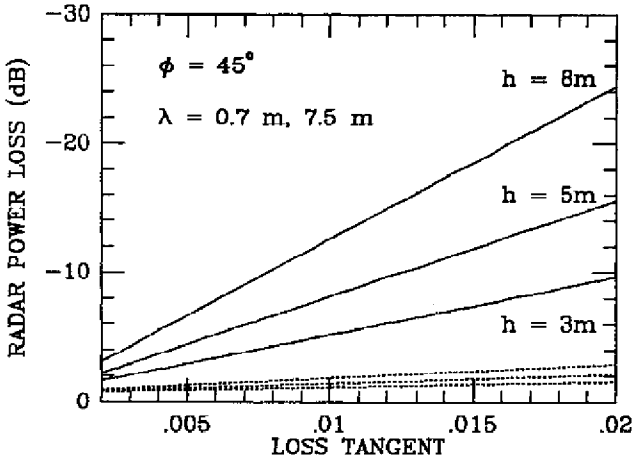

Figure 1. Change in backscatter cross section for a buried substrate as a function of layer depth, radar wavelength (70 cm, denoted by solid lines, and 7.5 m, denoted by dotted lines), and loss tangent for an incidence angle of 45°. Depth of regolith chosen to be 3, 5, and 8 m. Note that the dynamic range of substrate echoes for regolith depths >5 m over the possible loss tangent range is at least 10 dB, compared to the 8 dB range actually observed across the maria.

(about 8 dB, or a 6:1 ratio) across all of the nearside maria (Plate 1). The results illustrated in Figure 1 thus rule out substrate echoes as the sole contributor to the measured 70-cm backscatter, because regolith depths are likely to be greater than 3 m in the older maria [*Moore et al.*, 1980], and would lead to much larger variations in the backscatter strength with loss tangent than are observed. In reality, these large dynamic ranges will not be observed because some of the echo power comes from other mechanisms, such as Mie scattering. For deep regoliths, the round-trip 70-cm signal attenuation is strong enough to hide all but very rough buried surfaces. Losses due to attenuation for 7.5-m wavelength observations are <3 dB even for very high values of tanδ, and depend little upon regolith depth over the 3-8 m range.

Mie Scattering From Rocks

Another end-member model describes the regolith as a collection of rocks randomly distributed through a soil layer of given depth. These rocks are further distributed in size according to a power law relationship. A first-order estimate of the polarized backscatter cross section can be obtained by using Mie theory, assuming that only single scattering is important and neglecting shadowing of one rock by others [*Bohren and Huffman*, 1983]. *Thompson et al.* [1970] and *Pollack and Whitehill* [1972] tested the Mie scattering mechanism and concluded that returns from buried rocks were likely a major component of the 70-cm radar echoes, but they lacked calibrated data to carry the analysis to a local level. They further suggested that the primary cause of changes in the echoes, assuming a uniform rock population, was chemical (i.e., tanδ) variations in the regolith and that such changes could be used for geological mapping. The Pollack and Whitehill study also treated multiple scattering, and found that the average radar cross section and degree of polarization for the Moon could be modeled by a reasonable rock distribution. Their model is rather complicated in assuming that rocks are primarily found in concentric regions around parabola-shaped fresh young craters, but it ignores any depolarization by single scatter from non-spherical objects, does not treat the issue of regolith variations within a crater cavity, and takes a single rock population from the Tycho ejecta blanket as its test case. In this paper, we will examine just the Mie single-scattering model and compare its results to the 70-cm observations for the Surveyor landing sites.

A primary difference between the Mie scattering case and the substrate model discussed above is in the effect of the loss tangent on the echo. For a population of rocks randomly distributed in size throughout the soil layer, the net effect is to average the absorption over the total depth rather than to integrate along the large total path length from the surface to a buried substrate. We can write the total backscatter cross section as

$$\sigma^o = \frac{T^2}{4\alpha}\left[1 - e^{-4\alpha h/\cos\theta}\right]\int_{R_{min}}^{R_{max}} \sigma(r)\ p(r)\ dr \tag{6}$$

where $p(r)$ is the population density of rocks with radius r (in number/m^3), $\sigma(r)$ is the scattering cross section (m^2) for each rock derived from the Mie equations, and R_{min} and R_{max} are the range of rock sizes likely to produce 70-cm scattering (we integrate from 1 cm to 2 m). Note that the effect of h on σ^o in Eq. 6 is entirely contained in the exponential term, which disappears for large optical depths.

Rock populations for the lunar regolith are available from work done on the Surveyor landing site images by *Shoemaker and Morris* [1968], which were converted to differential probability functions by *Thompson et al.* [1970]. Volumetric populations can be obtained by equating the fractional area covered by surface rocks and the fractional volume occupied by buried rocks ("Rosiwal's principle", discussed by *Shoemaker and Morris* [1968]). From this approach, the differential volumetric rock population can be found from the surface distribution as

$$p(r) = \frac{3}{4} C_s\, r^{n-1} \tag{7}$$

where C_s is the coefficient of the surface differential rock power law and n is the exponent (both parameters vary from one landing site to another). Table 1 lists the power law fits for the Surveyor sites, showing that regions within the maria (all but Surveyor 7) can vary significantly in their behavior, presumably due to the relative proximity of young craters to each landing site. This table also includes the measured cross sections for each site from the calibrated 70-cm map.

We first calculated the total Mie backscatter cross section for just surface rocks at each Surveyor site and found that, even with a strong rock/soil dielectric contrast, scattering from only these rocks is at least 6 dB weaker than the observed LR echo strengths (Table 1). Only if the loss tangent of the surface rocks is allowed to drop to values of ~0.001 (where internal reflections within the rocks become very efficient) can we replicate the observed polarized cross section, and such low loss factors are plausible only for pure anorthositic (i.e., highlands) material. If we carry out the full volume-scattering calculation, considerably more echo power is predicted. Figure

Table 1. Volumetric Rock Population, Radar Incidence Angles, 70-cm Radar LR and LL Backscatter Coefficients, and Calculated Mie Surface Scattering Cross Sections for the Surveyor Lunar Landing Sites

Surveyor	Rock Population	Angle, deg	σ^{oLR}, σ^{oLL}, dB	Mie σ^o, dB
1	1400 $r^{-4.11}$	43	-21.6, -29.5	-32, -28
3	2700 $r^{-4.49}$	23	-15.1, -28.2	-34, -30
5	980 $r^{-4.63}$	23	-14.6, -28.1	-40, -36
6	2200 $r^{-4.52}$	-	-	-35, -31
7	4100 $r^{-3.82}$	42	-13.8, -16.0	-24, -20

Rock population values are in units of number/m^3, with radius in cm. Backscatter coefficients calculated for 10x10 km box surrounding each landing site. The Surveyor 6 site falls in the central data gap of the 70-cm map. The Mie cross sections assume only a surficial layer of rocks, with possible dielectric contrasts shown by the range in values (soil ε'=3, rock ε'=5-7; rock tanδ had little effect over the range 0.004-0.025). See text for discussion of volume scattering cross section.

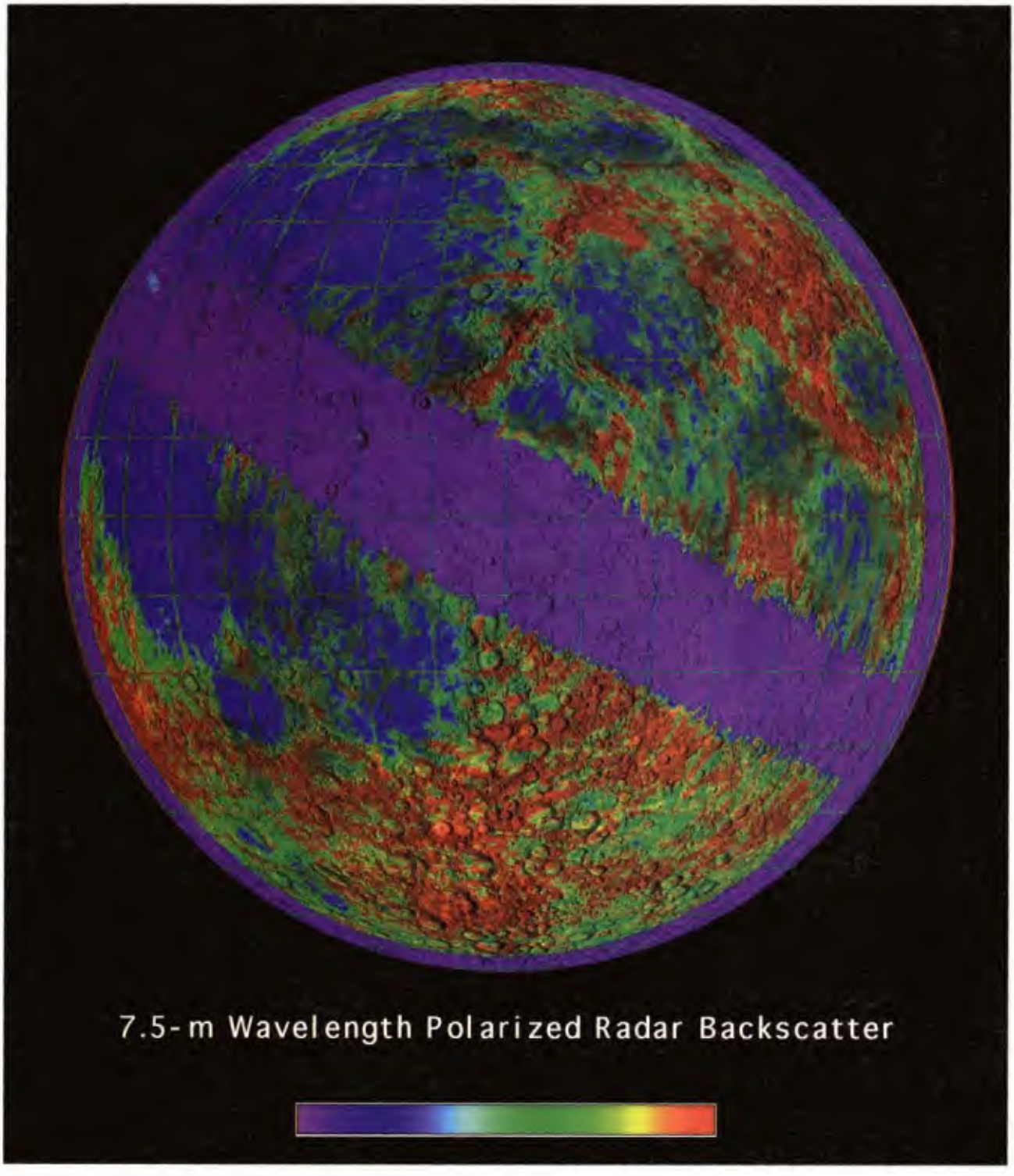

Plate 2. A 7.5-m radar image of the Moon [from *Thompson*, 1978], as a color overlay to the U.S. Geological Survey shaded-relief map. Orthographic projection; image resolution 30-50 km. Colors show logarithmic scaling of backscattered power relative to the lunar mean.

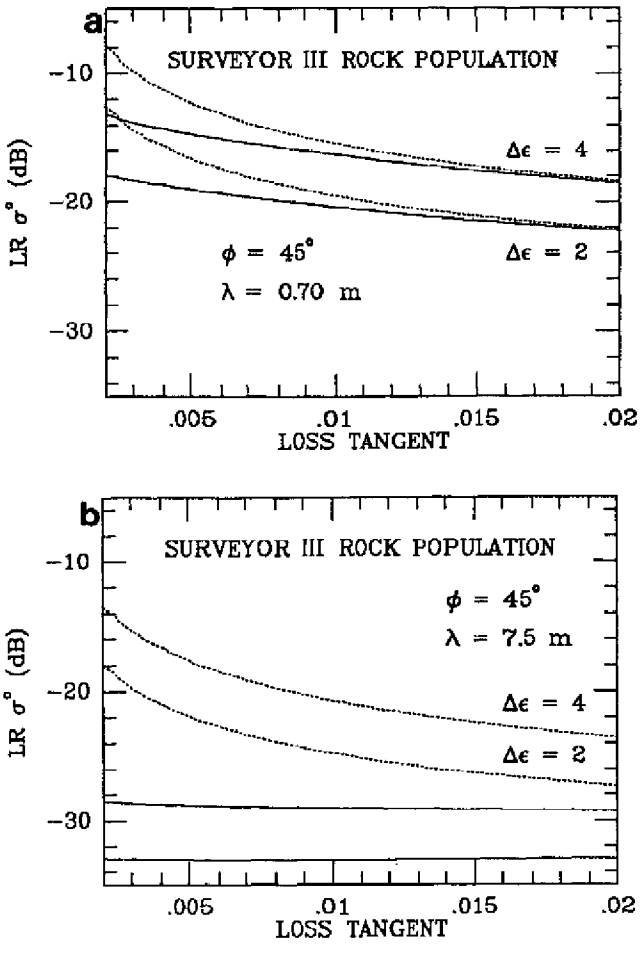

Figure 2. Volume scattering results based on Surveyor III rock population. Depth of the scattering layer is assumed to be 5 m (solid lines) and infinity (dotted lines). The higher backscatter values correspond to a rock/soil dielectric contrast of 4, while the lower values for each depth correspond to a contrast of 2. Results for radar wavelengths of (a) 70 cm and (b) 7.5 m shown.

2 shows the echoes found for volume scattering from (6) and the Surveyor III rock population, and demonstrates that even a low rock/soil dielectric contrast (ε'_{rock} = 5, ε'_{soil} = 3) and regolith depth of ~5 m can produce echoes consistent with the 70-cm polarized observations. Both results are in accord with those of *Thompson et al.* [1970], but it appears that multiple scattering is not necessarily required to produce the measured LR echo. A large component of subsurface Mie scattering is also consistent with the 12.6-cm lunar radar studies of *Stacy* [1993], who found that the echo from buried objects must be stronger in the polarized (LR) sense than in the depolarized mode. Mie scattering echoes from this rock population at 7.5-m wavelength are at least 5 dB lower than the 70-cm return, with greater differences for lower soil loss tangent (Figure 2b).

For a given rock population and fine-fraction loss tangent, the depth of the regolith determines the relative strength of the echo for this model (Figure 2). For example, at loss tangents >0.01, the regolith appears to the 70-cm radar to be bottomless (essentially infinite optical depth) for thicknesses of 5 m or more. With lower loss tangents, the effect of changes in depth on the observed return becomes very large. At the same time, low losses within the regolith favor echoes from the buried soil-rock interface. We will examine the effects of mixing the substrate and buried-rock returns below.

Depolarization

The depolarized (LL) radar echo, which we use below as a measure of diffuse scattering from the Moon, can be attributed to some combination of transmission effects through a dielectric interface (i.e., the soil surface), single-scattering by nonspherical objects, and multiple scattering between rocks suspended in the soil [*Hagfors*, 1967]. The first mechanism is not very efficient and, at most, produces only a few percent ellipticity in the received signal. The latter two mechanisms have the potential to produce significant depolarization, with the extreme case being that of randomly oriented small linear objects, which produce equal LL and LR returns. Polarization ratios (LL/LR) in the maria range from 0.05 to 0.40, increasing with incidence angle as the quasi-specular component of the LR return becomes less significant. Near the limb, *Hagfors* [1970] noted that the ratio was about 0.5, a value we used for calibration purposes.

Pollack and Whitehill [1972] showed that multiple-bounce radar returns could be a significant part of the total echo if the rock population is very high, such as in a crater ejecta blanket. It is difficult to judge the relative contributions of single and multiple scattering to the depolarized echo, however, since the shape of the rocks and the loss tangent of the regolith play a major role. We use primarily the LL echo strength to study the diffuse radar echo, but the specific mechanism of depolarization is not modeled. The Mie scattering mechanism discussed above does not predict the amount of depolarization for a nonspherical object, but we will assume that among the lunar maria there are no systematic differences in the shape of regolith clasts. In general, the total return should be a sum of many scattering events whose paths through the regolith and single-scattering albedoes (dependent mostly upon the real dielectric contrast) do not change with soil tanδ. As such, we expect the multiple-scattered component to scale linearly with any tanδ-induced changes in single-scattered energy.

Summary

The models above show that in all cases, increasing the loss tangent of the fine regolith fraction will lower the observed radar backscatter. The strength of the echo and its sensitivity to changes in tanδ are also affected, however, by the rock population, substrate roughness, and regolith depth. To explore the effects of mixing the substrate and buried-rock scattering mechanisms, we carried out a simulation using the rock population of the Surveyor III site. The real dielectric constant of rock and soil were taken to be 7 and 3, respectively, and we varied the regolith depth, tanδ, and the backscatter cross section of the substrate. Terrestrial lava flows have 68-cm LR backscatter coefficients of up to about -14 dB for very rough surfaces [*Campbell and Shepard*, 1996], so a value of -12 dB was used as a maximum plausible substrate cross section (allowing for potential multiple scattering if the substrate is blocky), prior to modification for the change in dielectric contrast, attenuation, and transmission losses.

The total backscatter calculated for this model is shown in Figure 3. The most significant result is that the substrate echo

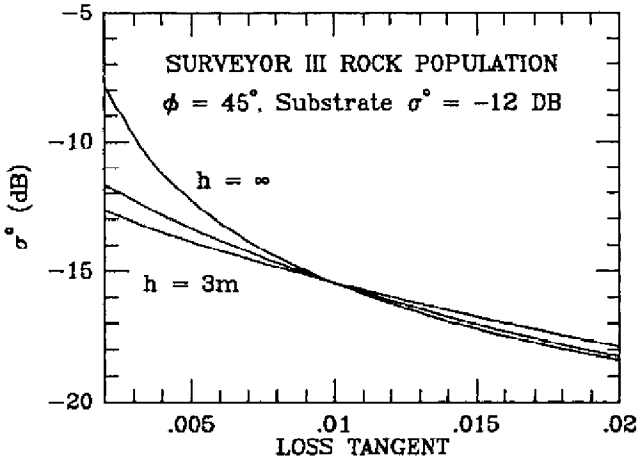

Figure 3. Modeled 70-cm radar echo for a lunar regolith with rock population corresponding to that of the Surveyor III site. Substrate radar echo (in the absence of a mantling layer) assumed to be -12 dB; rock and soil real dielectric constants assumed to be 7 and 3. Results for regolith depths of 3 m, 5 m, and infinite depth shown.

has no more than a 2 dB effect on the observed return, relative to the end-member Mie scattering model (Figure 2), even when the soil is shallow, the interface is rough, and tanδ is low. The range in echo strength with depth tends to be reduced by the inclusion of the substrate component, since the power lost in having a thinner mixed rock/soil layer is partially offset by the increasing visibility of the basal interface. Changes in regolith depth or substrate roughness are thus unlikely to cause the observed variations in 70-cm backscattering behavior between the maria.

The relative importance of different scattering mechanisms may vary from one site to another, and the interpretation of the radar data depends heavily on the assumed degree of heterogeneity in the vertical structure of the regolith over large areas. Variations in regolith depth and rock population with age are plausible, as are major shifts in the basalt loss tangent with varying elemental abundances. Changes of 3 dB or more are also possible in the Mie scattering model for reasonable shifts in the real dielectric constant (i.e., the density) of the buried rocks (ε'=5-7), but over the maria we can likely choose a single mean value for rock density which will not vary systematically from one basalt flow complex to the next.

Measured variations in rock population are quite large among the Surveyor I, III, V, and VI sites, leading to a 5-8 dB range in predicted radar volume scattering. The lack of a similar large shift in the observed echoes from the various sites (Surveyor V is actually slightly brighter relative to the lunar mean than Surveyor I) suggests that these local rock counts do not necessarily indicate regional differences in regolith structure, but rather the proximity of small young craters to the landing sites. Infrared eclipse brightness temperatures for the maria (Figure 4) show, however, that the

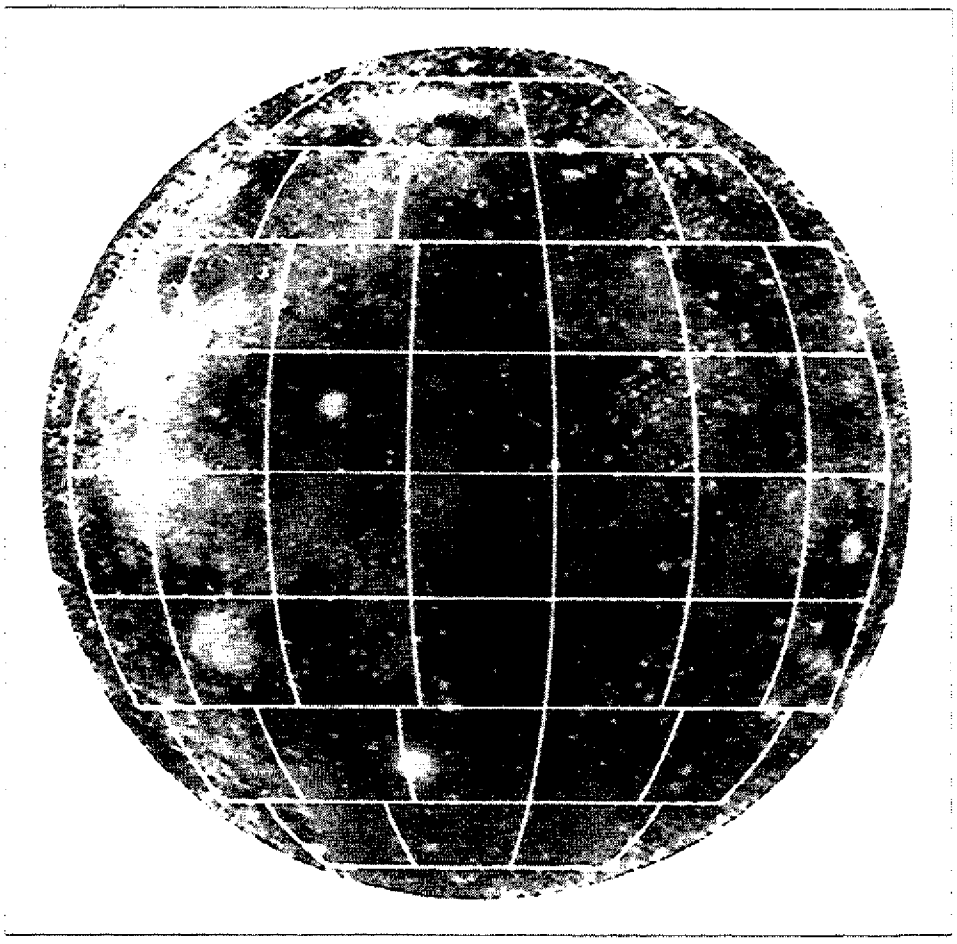

Figure 4. Thermal infrared eclipse image of the Moon [from *Shorthill*, 1973]. Brighter areas have higher surface rock abundance or more granular soil.

Imbrium and Procellarum basalts have higher eclipse temperatures than the older Serenitatis and Tranquilitatis materials, implying a higher surface population of rocks or a more granular particulate surface soil [*Shorthill*, 1973; *Moore et al.*, 1980]. In the next section, we attempt to further constrain the possible scattering mechanisms, and thus regolith properties, by comparing the radar data to multispectral estimates of mare elemental abundances.

Comparison of 70-cm Radar and Multispectral Data

We first chose several sample sites within each of six nearside maria (Imbrium, Procellarum, Serenitatis, Tranquilitatis, Fecunditatis, and Crisium) to illustrate the range of echo strengths across these regions. Each site was selected to sample only one type of basaltic unit as defined by *Pieters* [1978] and to avoid the ejecta blankets of large craters. Estimates of TiO_2 abundance were taken from the published maps of *Johnson et al.* [1991] and *Lucey et al.* [1996], who derived these values using differing spectral-ratio techniques. The FeO abundance values of *Lucey et al.* [1995] were also averaged for each area. The 70-cm depolarized data were normalized prior to averaging for the $\cos\phi$ dependence of projected area on incidence angle. The locations of these sites are presented in Figure 5, and Figure 6 shows summary plots of the mare remote sensing data.

Comparison of 70-cm depolarized radar backscatter values to FeO abundance from *Lucey et al.* [1995] shows no correlation across the maria (Figure 6a). While FeO is a major constituent of ilmenite, it is also found in a variety of other minerals which do not apparently affect the microwave loss tangent; iron content has no systematic correlation with ilmenite abundance in lunar basalts [*Papike et al.*, 1991]. Small grains of reduced Fe in agglutinates are likewise not a major source of $\tan\delta$ variability. The inferred correlation of loss tangent on total $FeO+TiO_2$ abundance from lab studies may thus be reflective of just the ilmenite component of the samples.

The comparison of TiO_2 and radar backscatter reveals several interesting results. The depolarized echo power is anticorrelated with titanium abundance for Mare Imbrium (Figure 6b), consistent with the observations of *Schaber et al.* [1975]. This relationship is better defined for the *Lucey et al.* [1996] TiO_2 data (Figure 6b), which appear to provide more robust estimates of elemental abundance at very low values (<3%) than the ratio method proposed by *Charette et al.* [1974] and used in the *Johnson et al.* [1991] map (Figure 6d). A similar negative correlation is observed for Oceanus Procellarum, Mare Tranquilitatis, and Mare Fecunditatis. Maria Serenitatis and Crisium have more narrow ranges of TiO_2 abundance at the scales of interest here, which makes the analysis of possible trends between backscatter and elemental composition difficult (Figure 6c).

To better characterize any possible dependence of radar echo on TiO_2 content, we created image masks for the six maria of interest, which excluded the surrounding highlands and many large, radar-bright craters. The average backscatter as a function of *Lucey et al.*'s [1996] TiO_2 abundance was then calculated (Figure 7). This plot shows that there is a consistent negative correlation between 70-cm echo power and titanium content across the lunar maria. The echoes for Mare Crisium, Mare Imbrium, and Oceanus Procellarum exhibit a more rapid increase at very low TiO_2 contents than returns from the other regions. There are also significant offsets in absolute echo power between the maria, with a total spread of ~3 dB. For example, Mare Fecunditatis is systematically more radar-dark for a given TiO_2 value than the Mare Imbrium deposits, while Mare Tranquilitatis is brighter for any given titanium abundance (greater than ~1%) relative to Imbrium.

How do we reconcile the radar and multispectral observations? The radar sample sites (Figures 6 and 7) show that the relationship between σ^0 and TiO_2 can change from one basin to another, and perhaps even within any single mare complex. We could attribute these differences to several possibilities: (1) systematic offsets between the images used to create the final radar map, (2) dependence of the radar echo on minerals other than ilmenite, (3) age-related variations in rock population between the maria, or (4) variations in regolith depth with age.

Some of the brightness change for Mare Tranquilitatis may be due to power "folded in" from conjugate regions, due to the north-south ambiguity inherent in these radar observations. In this case the strong echo is from Tycho, which appears as a diffuse bright streak across the central portion of the basin in Figure 5c. No similar explanations can be made for the other offsets seen in Figure 7, but we cannot rule out some component of slight mosaicking offsets or power scattered by conjugate areas. The data shown in Figures 6 and 7 have been normalized to a $\cos\phi$ scattering law, but if the local surface behaves differently then we will incur an additional small error. The possibility that the microwave loss tangent is modulated by other mineralogic components unrelated to the TiO_2 (i.e., ilmenite) abundance is unsupported at present, given laboratory studies and the observed absence of any correlation between backscatter and FeO content [*Carrier et al.*, 1991].

The other two alternatives, rock population and depth changes, are interrelated and can be tested against the results of other remote-sensing studies. Thermal infrared eclipse images, geologic mapping, crater morphology analysis, and crater population data all imply that, of our study regions, Mare Imbrium and Oceanus Procellarum contain the youngest mare basalt flows [*Shorthill*, 1973; *Boyce and Johnson*, 1978]. These younger surfaces are characterized by a higher population of small rocks at the surface, possibly indicating a thin regolith which permits smaller impactors to excavate competent material (Figure 4). Mare Tranquilitatis contains the oldest basalt flows, with Mare Crisium exhibiting a wide range in apparent surface age. Maria Fecunditatis and Serenitatis represent progressively younger materials, intermediate in age between Maria Tranquilitatis and Imbrium [*Boyce and Johnson*, 1978]. Shifts in echo power between deposits of the various basins may thus be attributable to differences in the rock population with age. For example, if the Mare Fecunditatis basalts are indeed older than those of Mare Imbrium, then the regolith may be less rocky in this area, leading to lower diffuse backscatter. This model does not, however, explain all of the differences between the six mare regions we studied (Figure 7).

Our observations show that, consistent with earlier studies of Mare Imbrium, the TiO_2 (ilmenite) content of the regolith has a significant effect on the observed backscatter strength, with higher titanium abundance leading to lower radar echoes. We expect that the radar return is also controlled by the average rock population within the lunar soil, such that younger mare units will have systematically higher 70-cm

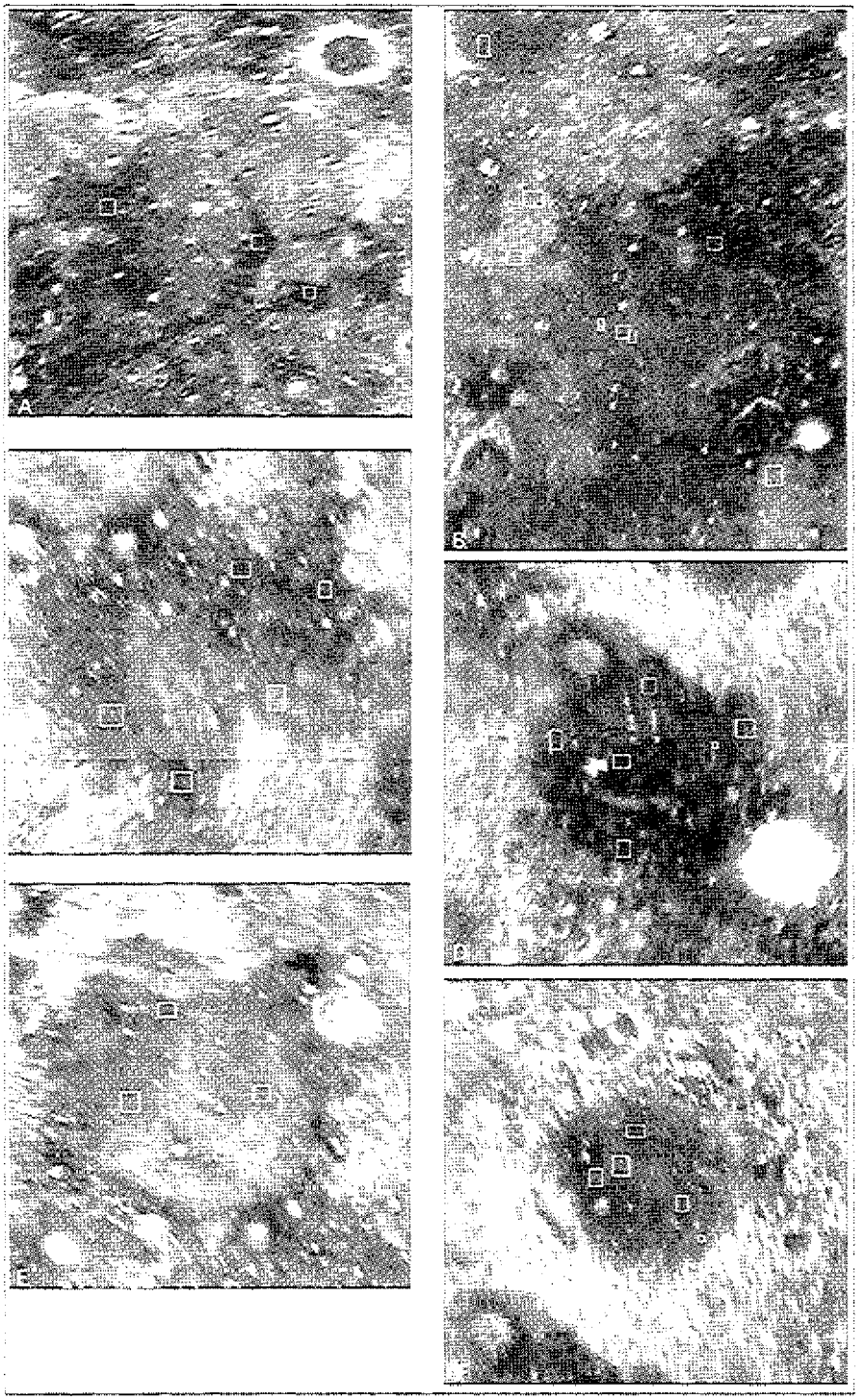

Figure 5. Locations of sample boxes for remote sensing data comparison. All maps are simple cylindrical projections of 70-cm depolarized radar data. (a) Mare Imbrium. Image area 25°-55°N, 325°-355°E. (b) Oceanus Procellarum. Image area 15°-55°N, 285°-315°E. (c) Mare Tranquilitatis. Image area 15°-45°N, 353°-23°E. (d) Mare Fecunditatis. Image area 17°S - 13°N, 36°-66°E. (e) Mare Serenitatis. Image area 12°-42°N, 5°-35°E. (f) Mare Crisium. Image area 2°-32°N, 43°-73°E.

returns than older deposits due to a greater number of surface and buried rocks. While the properties of Mare Fecunditatis are possible evidence for such behavior, the data shown here cannot be used to further test this hypothesis, due to uncertainties regarding calibration and N-S image ambiguity.

Analysis of 7.5-m Radar Data

The 7.5-m wavelength radar image (LR polarization only) was collected in 1977 at the Arecibo Observatory, and has a resolution of 30-50 km [*Thompson*, 1978]. Since the original

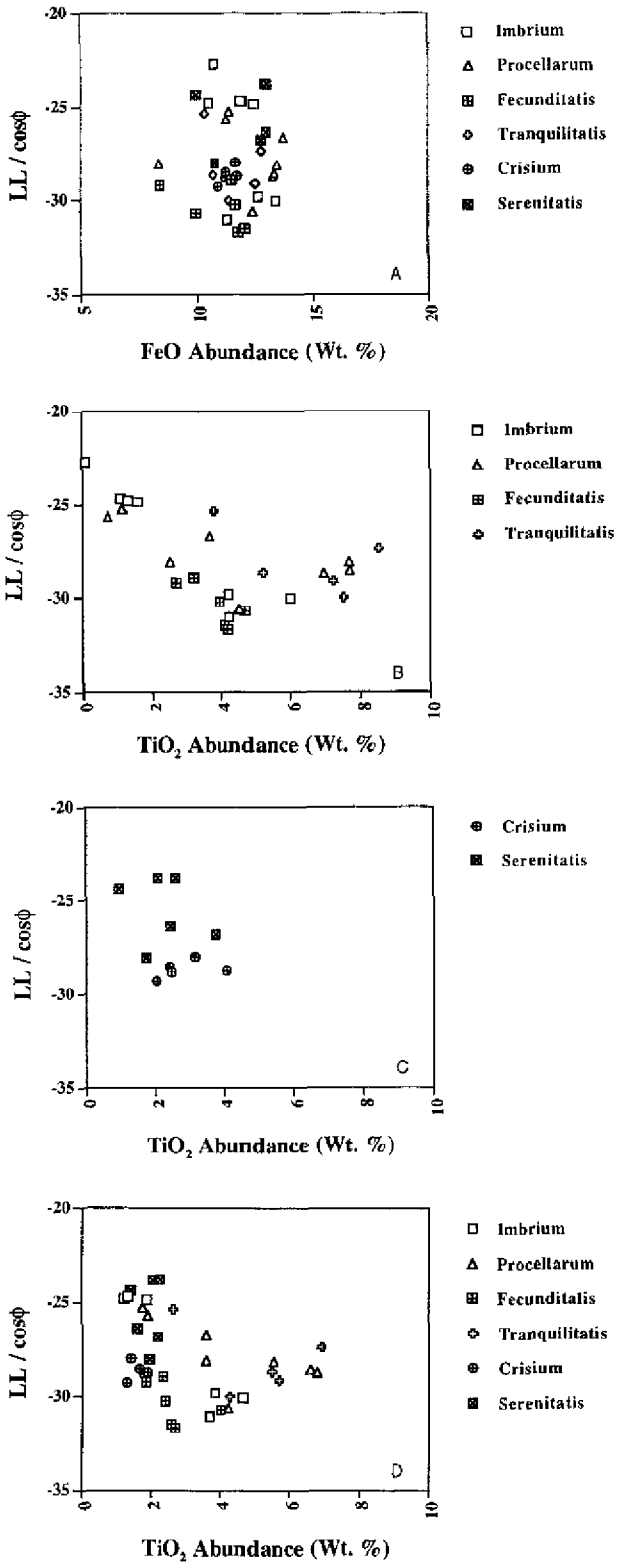

Figure 6. (a) Plot of normalized LL radar echo (dB) versus FeO content [*Lucey et al.*, 1995]. (b) Plot of normalized LL radar echo (dB) versus TiO_2 content [*Lucey et al.*, 1996] for Maria Imbrium, Fecunditatis, Tranquilitatis, and Occanus Procellarum. (c) Plot of normalized LL radar echo (dB) versus TiO_2 content [*Lucey et al.*, 1996] for Maria Crisium and Serenitatis. (d) Plot of normalized LL radar echo (dB) versus TiO_2 content [*Johnson et al.*, 1991].

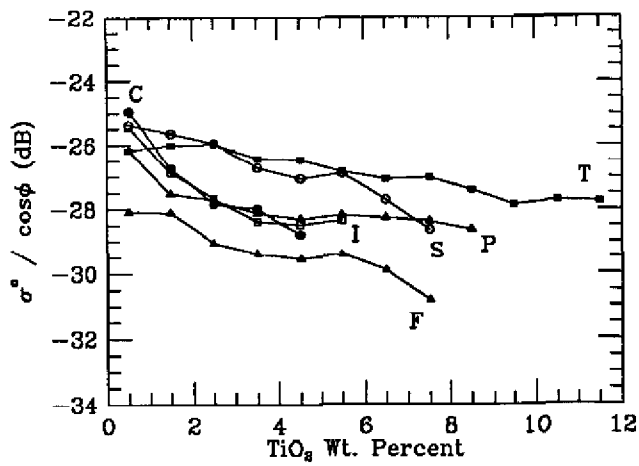

Figure 7. Plot of average depolarized radar echo strength as a function of titanium abundance [*Lucey et al.*, 1996] for six mare regions: Mare Tranquilitatis (T), Mare Fecunditatis (F), Mare Imbrium (I), Mare Serenitatis (S), Mare Crisium (C), and Oceanus Procellarum (P). Radar echoes normalized to the cosine of the incidence angle prior to averaging.

data were unavailable, the map was recovered by digitally scanning a photo negative and putting the image into a cartographic framework (Plate 2). The registration of the radar image and base map are relatively good near the center of the Moon, but there are positional errors near the limbs, so we did not attempt any reprojections of the data. The very long radar wavelength will penetrate a considerable distance into the subregolith basalt, and the paucity of scatterers within the regolith at the wavelength scale means that the soil/rock layer plays little role in the final return (Figures 1 and 2b). For the maria, these data thus reflect the scattering and absorption properties of the basalt layers below the soil.

The behavior of the 7.5-m radar data for the maria is often not well matched with the 70-cm results. Since 70-cm backscatter was shown to correlate well with TiO_2 variations, we infer that ilmenite abundance within the regolith and basal lava flows does not greatly affect the 7.5-m echoes. Mare Serenitatis, seen at 70 cm to be one of the brightest mare surfaces, has very low 7.5 returns in the southwestern half of the basin. This contrasts with the echoes from Mare Tranquilitatis, which despite its high TiO_2 content is the brightest mare at 7.5 m. Mare Fecunditatis and Mare Crisium have intermediate 7.5-m backscatter, whereas Fecunditatis has the lowest 70-cm returns of any large mare. The lowest 7.5 m echoes on the Moon are associated with the Imbrium, Humorum, and Procellarum mare deposits.

Infrared eclipse temperature (Figure 4) and 7.5-m backscatter power are consistently anticorrelated; the low radar returns from the western nearside maria are associated with the younger age and greater surface rock abundance of these deposits, while the older eastern mare basalts tend to have fewer surface rocks and higher 7.5-m backscatter power [*Shorthill*, 1973; *Thompson*, 1978]. If we assume that variations in the loss tangent of the fine regolith component are not modulating the 7.5-m mare scattering, then what properties of the substrate basalts would lead to these behaviors? If the younger flow units on the western nearside

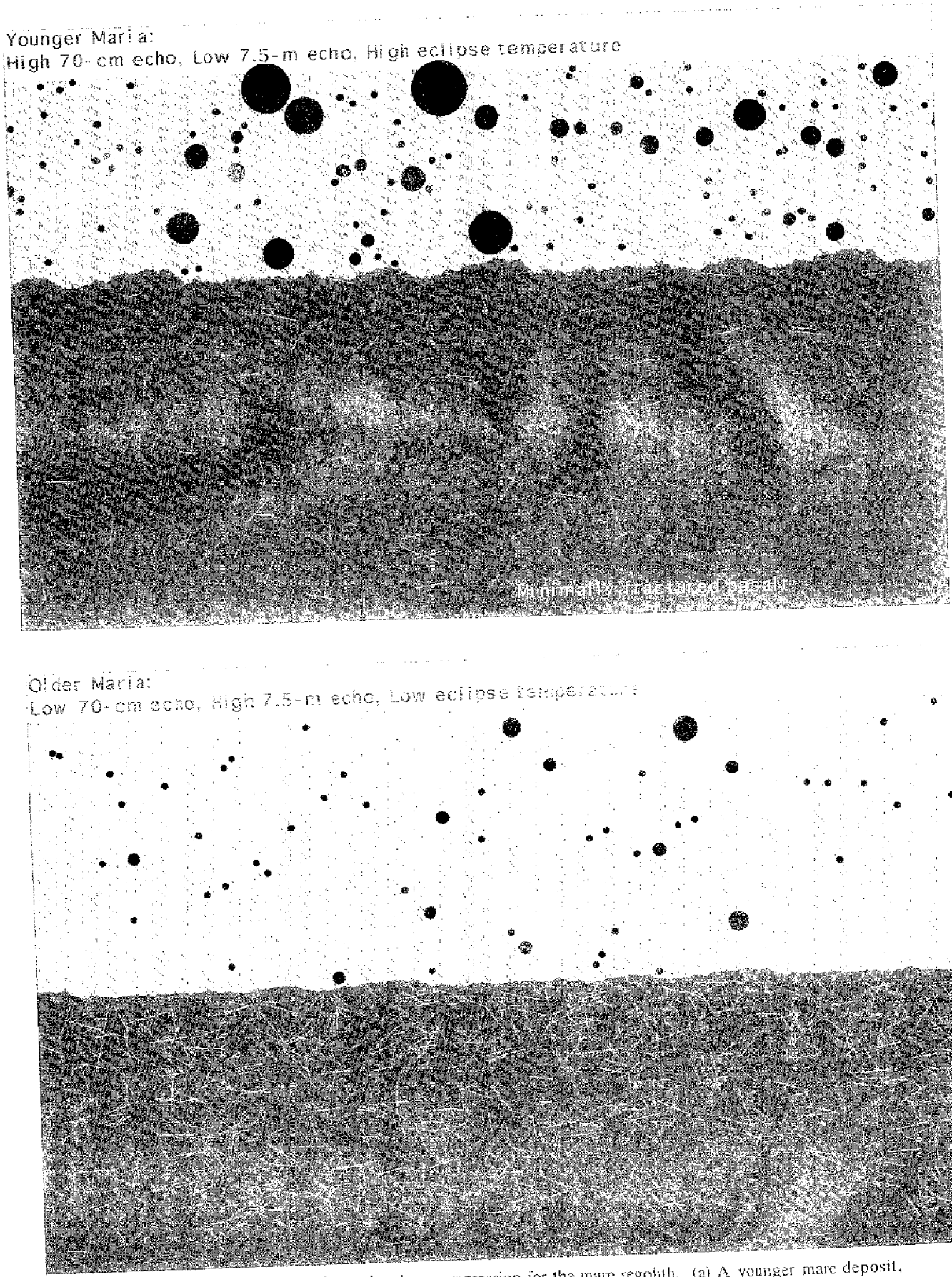

Figure 8. Schematic views of postulated age progression for the mare regolith. (a) A younger mare deposit, characterized by a thin soil layer, high volumetric rock population, and limited fracturing of the underlying basalt flows. (b) An older mare unit, with greater soil depth, lower rock abundance, and a high degree of fracturing within the underlying basalts.

have less developed regoliths, then the degree of deep fracturing and brecciation within the basalt layers may be less than that for older mare deposits. This would lead to fewer discontinuities within the rock, and consequently less volume scattering of energy passing though the stack of lava flows beneath the regolith. By analogy, the high 7.5-m radar return from the lunar highlands is attributable to scattering from large blocks at significant depths within the low-loss anorthositic megaregolith [*Thompson*, 1978].

Discussion

These results imply several conclusions. (1) The 70-cm radar echo for the maria comes largely from Mie scattering by rocks buried within the fine soil. Radar scattering by a buried substrate is not likely to greatly affect the observed return. (2) The TiO_2 (ilmenite) content of the regolith controls variations in 70-cm depolarized echo strength among mare units of similar age. (3) Changes in the absolute value of the 70-cm return between maria of different ages are expected to reflect the variations in surface and buried rock population indicated by infrared eclipse maps. Some of our results are consistent with this model, but additional calibrated observations are necessary for any further analyses. (4) The 7.5-m radar echoes are controlled by the age of the mare basalt flows, with older deposits having a greater degree of fracturing and higher backscatter.

Figure 8 illustrates a postulated age-progression for the lunar mare regolith. Younger basalt units (Figure 8a) have thinner fine-grained soil cover, greater volumetric rock population, and a smaller degree of shattering and brecciation within the underlying stack of flows. This leads to a predicted high 70-cm echo, a low 7.5-m return, and high eclipse temperatures. With increasing age (Figure 8b), the depth of the fine-grained soil increases, and impact gardening reduces the size and number of included rocks. The greater number of total accumulated impacts for older units leads to a high degree of fracturing within the basal flows. The result is low 70-cm echoes, high 7.5-m backscatter, and low eclipse temperatures.

Future work will focus on comparing the 70-cm radar echoes to local changes in elemental abundance, and on the investigation of anomalous regions. Observations at this wavelength with resolution as fine as 300 m are possible from Arecibo, so new work will be carried out to image areas of particular interest and to resolve the issue of age-dependent changes in rock population and 70-cm echo. Additionally, mapping at 12.6-cm wavelength will permit an assessment of the Mie scattering model and the possible changes in rock population between the maria. These data provide a valuable complementary tool to multispectral techniques, and it is expected that much can be gained from their synthesis.

Acknowledgments. The authors thank Haig Morgan at the USGS for scanning the 7.5-m radar image, Jeffrey Johnson for providing the digital TiO_2 maps, and Paul Lucey for digital versions of his iron and titanium maps. Thanks also to Ted Maxwell and two anonymous reviewers for helpful comments. This work was supported in part by NASA PG&G grant NAGW-3360 and a grant from the Lunar and Asteroid data analysis program (B.A.C.). The research conducted by T.W.T. was performed at the Jet Propulsion Laboratory, California Institute of Technology, under a contract with NASA.

References

Bohren, C.F., and D.R. Huffman, *Scattering and Emission From Small Particles*, John Wiley, New York, 1983.

Boyce, J.M., and D.A. Johnson, Ages of flow units in the far eastern maria and implications for basin-filling history, *Lunar Planet. Sci. Conf. IX*, 3275-3284, 1978.

Campbell, B.A., and M.K. Shepard, Lava flow surface roughness and depolarized radar scattering, *J. Geophys. Res., 101*, 18,941-18,952, 1996.

Carrier, W.D., G.R. Olhoeft, and W. Mendell, Physical properties of the lunar surface, in *Lunar Sourcebook*, Cambridge Univ. Press, New York, 1991.

Charette, M.P., T.B. McCord, C. Pieters, and J.B. Adams, Applications of remote spectral reflectance measurements to lunar geology classification and determination of titanium content of lunar soils, *J. Geophys. Res., 79*, 1605-1613, 1974.

Davis, P.A., Iron and titanium distribution on the Moon from orbital gamma ray spectroscopy with implications for crustal evolutionary models, *J. Geophys. Res., 85*, 3209-3224, 1980.

Gaddis, L.R., C.M. Pieters, and B.R. Hawke, Remote sensing of lunar pyroclastic mantling deposits, *Icarus, 61*, 461-489, 1985.

Hagfors, T., Remote probing of the Moon by infrared and microwave emissions and by radar, *Radio Sci., 5*, 189-227, 1970.

Hagfors, T., A study of the depolarization of lunar radar echoes, *Radio Sci., 2*, 445-465, 1967.

Horz, F., R. Grieve, G. Heiken, P. Spudis, and A. Binder, Lunar surface processes, in *Lunar Sourcebook*, Cambridge Univ. Press, New York, 1991.

Johnson, J.R., S.M. Larson, and R.B. Singer, Remote sensing of potential lunar resources 1. Near-side compositional properties, *J. Geophys. Res., 96*, 18,861-18,882, 1991.

Lucey, P.G., D.T. Blewett, J.L. Johnson, G.J. Taylor, and B.R. Hawke, Lunar titanium content from UV-VIS measurements (absrract), *Lunar Planet. Sci. Conf. XXVII*, 781-782, 1996.

Lucey, P.G., G.J. Taylor, and E, Malaret, Abundance and distribution of iron on the Moon, *Science, 268*, 1150-1153, 1995.

Melendrez, D.E., J.R. Johnson, S.M. Larson, and R.B. Singer, Remote sensing of potential lunar resources, 2; High spatial resolution mapping of spectral reflectance ratios and implications for nearside mare TiO_2 content, *J. Geophys. Res., 99*, 5601-5620, 1994.

Moore, H.J., J.M. Boyce, G.G. Schaber, and D.H. Scott, Lunar remote sensing and measurements, *U.S. Geological Survey Prof. Pap. 1046-B*, 1980.

Olhoeft, G.R., and D.W. Strangway, Dielectric properties of the first 100 m of the Moon, *Earth Planet. Sci. Lett., 24*, 394-404, 1975.

Papike, J., L. Taylor, and S. Simon, Lunar minerals, in *Lunar Sourcebook*, Cambridge Univ. Press, New York, 1991.

Pieters, C., Mare basalts on the front side of the moon: A summary of spectral reflectance data, *Proc.9th Lunar Planet. Sci. Conf.*, 2825-2849, 1978.

Pieters, C.M., et al., Crustal diversity of the Moon: Compositional analyses of Galileo SSI data, *J. Geophys. Res., 98*, 17127-17148, 1993.

Pollack, J.B., and L. Whitehill, A multiple-scattering model of the diffuse component of lunar radar echoes, *J. Geophys. Res., 77*, 4289-4303, 1972.

Schaber, G.G., T.W. Thompson, and S.H. Zisk, Lava flows in Mare Imbrium: An evaluation of anomalously low Earth-based radar reflectivity, *Moon, 13*, 395-423, 1975.

Shoemaker, E.M., and E. Morris, Size distribution of fragmental debris, in Surveyor Project Final Report, Part 2, *JPL Tech. Rep., 32-1265*, 86-102, 1968.

Shorthill, R.W., Infrared atlas charts of the eclipsed Moon, *Moon*, 7, 22-45, 1973.

Stacy, N.J.S., High-resolution synthetic aperture radar observations of the Moon, Ph.D. dissertation, Cornell Univ., Ithaca, New York, 1993.

Stratton, J.A., *Electromagnetic Theory*, John Wiley, New York, 1947.

Thompson, T.W., Atlas of lunar radar maps at 70-cm wavelength, *Moon, 10*, 51-85, 1974.

Thompson, T.W., High resolution lunar radar map at 7.5-m wavelength, *Icarus, 36*, 174-188, 1978.

Thompson, T.W., High-resolution lunar radar map at 70-cm wavelength, *Earth Moon Planets, 37*, 59-70, 1987.

Thompson, T.W., J.B. Pollack, M.J. Campbell, and B.T. O'Leary, Radar maps of the Moon at 70-cm wavelength and their interpretation, Radio Science, 5, 253-262, 1970.

Thompson, T.W., W.J. Roberts, W.K. Hartmann, R.W. Shorthill, and S.H. Zisk, Blocky craters: Implications about the lunar mega-regolith, *Moon Planets, 21*, 319-342, 1979.

Ulaby, F.T., R.K. Moore, and A.K. Fung, *Microwave Remote Sensing*, Addison-Wesley, Reading, Mass., 1987.

Ulaby, F.T., T. Bengal, J. East, M.C. Dobson, J. Garvin, and D. Evans, Microwave dielectric spectrum of rocks, *Rep. 23817-1-T*, Univ. of Mich. Radiat. Lab, Ann Arbor, 1988.

Whitaker, E.A., Lunar color boundaries and their relationship to topographic features: A preliminary survey, *Moon, 4*, 348-355, 1972.

Wilhelms, D.E., The geologic history of the Moon, *U.S. Geological Survey Prof. Pap., 1348*, 1987.

Zisk, S.H., G.H. Pettengill, and G.W. Catuna, High-resolution radar maps of the lunar surface at 3.8-cm wavelength, *Moon, 10*, 17-50, 1974.

Zisk, S.H., C.A. Hodges, H.J. Moore, R.W. Shorthill, T.W. Thompson, E.A. Whitaker, and D.E. Wilhelms, The Aristarchus-Harbinger region of the Moon: Surface geology and history from recent remote-sensing observations, *Moon, 17*, 59-99, 1977.

B. A. Campbell, Center for Earth and Planetary Studies, MRC 315, Smithsonian Institution, Washington, DC 20560. (e-mail: campbell@ceps.nasm.edu)

B.R. Hawke, Department of Planetary Geosciences, University of Hawaii, 2525 Correa Road, Honolulu, HI 96822.

T.W. Thompson, Jet Propulsion Laboratory, Pasadena, CA 91109.

(Received July 27, 1995; revised March 11, 1997;
accepted March 17, 1997.)